COMBINED THERMO-ACOUSTIC UPGRADING OF SOLID FUEL: EXPERIMENTAL AND NUMERICAL INVESTIGATION

Luiz Gustavo O. Galvão [a], Bruno S. Chaves [a], Marcus Vinícius Girão de Morais [b], Ailton T. do Vale [c],
Armando Caldeira-Pires [b], Patrick Rousset [d] , Edgar A. Silveira [b]
a. Forest Products Laboratory (LPF), Brazilian Forest Service (SFB), Brasilia DF, 70818-900, Brazil
b. Mechanical Engineering Department, University of Brasília, Brasília, DF 70910-900, Brazil
c. Forest Engineering Department, University of Brasília, Brasília, DF 70910-900, Brazil
d. French Agriculture Research Centre for International Development (CIRAD), 73 rue J. F. Breton, 34398 Montpellier, Cedex 5, France

ABSTRACT: Torrefaction is a thermal modification used to the enhancement of fuel characteristics. This paper describes the effect of an innovative thermo-acoustic torrefaction reactor on the physical and chemical properties of torrefied *Eucalyptus grandis* wood. The aim was to evaluate the combined effect of the temperature (250 and 270 °C) and acoustic frequencies (1411,1810,2478 and 2696 Hz) by the assessment of the solid yield and its deviation, proximate and elemental analysis as well as energy content. A numerical model of kinetics reaction rates and solid composition allowed the evaluation of the thermo-acoustic torrefaction experiment showing faster reaction rates for treatments under acoustic. Statistical analysis results indicated that the applied frequencies affect the higher heating value but did not significantly affect the other parameters. However, its dynamic profiles show that acoustic may accelerate the degradation process. The kinetic numerical simulation of the acoustic coupling resulted in faster conversion rates for the solid pseudo-components leading to a stronger degradation of the intermediate product.
Keywords: Torrefaction, biomass, eucalyptus, catalytic conversion, modelling

1 INTRODUCTION

Many efforts in developing renewable energy and alternative fuels have been carried out to address the challenges of increasing global population, environmental pollution, and high greenhouse gas (GHG) emissions [1].

Biomass is one of the promising clean and green fuel, appropriate for daily energy requirements [2]. However, biomass needs a conversion process to overcome the inherent drawbacks as high moisture content, low calorific value, hygroscopic nature, low bulk density, which result in low conversion efficiency as well as difficulties in its collection, grinding, storage and transportation [1].

In recent years, torrefaction has received significant attention from both researchers and industries because of its potential to improve the biomass properties to a level comparable with coal [3]. In general, the torrefaction process is carried out in the temperature range of 200–300 °C, at slow heating rates [3] and usually performed in two atmospheres: nitrogen and oxygen [4] to produce a solid fuel more homogeny, hydrophobic and with a higher carbon content when compared to the raw material [1,5].

Several types of reactors are used for biomass torrefaction. Some of the reactors fall under one of the following types: (i) fixed bed, (ii) microwave, (iii) rotary drum, and (iv) fluidized bed [6]. Regarding fixed bed reactors technologies as a vacuum atmosphere, wet-torrefaction [7–10], as well as catalytic effects with biomass salt impregnation and doping [11–13], have been explored to improve the thermal pre-treatment.

An acoustic wave device was attached to a torrefaction reactor and is described in [14]. This study showed that temperature coupled to acoustic frequencies reported faster conversion rates during solid yield evolution [14].

Considering these results, this study intended to evaluate the effect of thermoacoustic torrefaction by the assessment of chemical properties. The proximate, elemental, and calorific analysis, as well as kinetic modeling, were conducted to examine the torrefied product.

2 MATERIAL AND METHODS

2.1 Material

A controlled growing tree of *Eucalyptus grandis* was cut into 3 cm^3 cubes with roughly the same density. Samples were dried in an oven at 105 °C for 24 h before the experiments. The proximate and ultimate analyses, as well as energy content values for the raw material, are shown in Table I.

Table I: Proximate, elemental, and calorific analyses of Eucalyptus grandis.

Raw material	*Eucalyptus grandis*
Physical appearance	
Proximate analysis [a]	
Fixed carbon	18.51
Volatile matter (VM)	81.4
Ash	0.09
Elemental analysis [a]	
C	46.03
H	6.19
N	0.13
O [b]	47.65
HHV (MJ kg^{-1})	20.09

[a] Dry basis, [b] O (wt%) = 100–C–H–N–Ash

2.2 Reactor system

The thermo acoustic laboratory-scale reactor system [14] is illustrated in Fig. 1. The reactor included a square chamber with two internal electrical heaters. Oxygen concentration (10%) was maintained by N_2 injection. The reaction temperature was controlled by a proportional integral derivative (PID) temperature controller based on a PT100 placed in the middle of the reactor to record the atmosphere temperature. A *Sartorius LP2200S* balance with an accuracy of 10^{-3} g records the sample weight. The system provides continuous acquisition data with a 100 Hz

sampling rate (*e.bloxx A4-1TC Multichannel*) recording mass weight during the wood heat treatment.
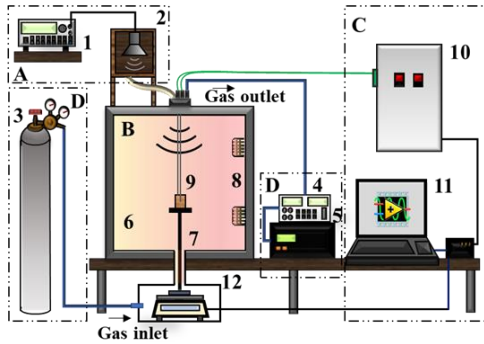

Figure 1: General diagram of the experimental torrefaction system: 1) Wave generator; 2) Sound speaker 3) N2 cylinder; 4) Gas pump; 5) O_2 control; 6) Reactor chamber; 7) Wood sample support; 8) Electric resistances for convection heating; 9) Thermocouples; 10) System control; 11) Computer; 12) Electric weight balance [14].

The desired and identified frequencies in [14] were produced by an *HP 33120A* wave generator and one *Selenium D220TI 8* speaker connected by a flexible duct [15] to the reactor cavity to deliver the acoustic wave inside the reactor. Data were sent to a computer to control the reaction temperature and the nitrogen percentage, and record wood surface and core temperature profiles and mass loss during heat treatment with and without acoustic influence [14].

2.3 Experimental procedure

The samples were linear heate (5 °C.min^{-1}) until the desired temperature of 250 or 270 °C [14]. Thereafter, they were torrefied for 60 minutes [14]. The carrier gas was continuously delivered into the reaction chamber to keep the system in a controlled oxygen concentration (10 % O_2) and remove volatiles produced during the torrefaction within the reactor [14]. The torrefaction treatment parameters are listed in Table II.

Table II: Thermo-acoustic torrefaction parameters.

Torrefaction conditions			
Duration	HR[a]	Atm.[b]	Temp/frequency
60 min	5°C.min^{-1}	10% O_2	250°C [a] / -
			250°C / 1411 Hz
			250°C / 1810 Hz
			250°C / 2478 Hz
			250°C / 2696 Hz
			270°C [a] / -
			270°C / 1411 Hz
			270°C / 1810 Hz
			270°C / 2478 Hz
			270°C / 2696 Hz

[a] Heating rate, [b] Atmosphere

The experiments conducted without acoustic influence (only thermal treatment) served as control [14]. The other experiments were conducted for both temperatures

coupled to 1411, 1810, 2478 and 2696 Hz acoustic frequencies held throughout the complete experimentation [14]. Those frequencies were identified in [14] and, within the system limits, have the power to produce the maximum particle velocity around the wood sample affecting the interaction between gaseous environment and wood surface [14]. For a statistical purpose, three experiments were performed for each condition. The analysis of the torrefied solid product allowed the catalytic effect of thermo-acoustic torrefaction.

2.4 Torrefied solid product analysis

The elemental analysis was conducted according to the American Society for Testing and Materials (ASTM E777 e E778) with a Perkin Elmer EA 2400 series II elemental analyzer, to detect the weight percentages of C, H, N for raw and torrefied biomass [16,17]. The oxygen content was calculated by difference [1]. Proximate analyses (fixed carbon, volatile matter, and ash contents) were performed with the standard procedure of the ASTM D3172 – 13 [16,17]. The calorific values of raw and torrefied biomass samples were measured according to the standard ASTM D5865 with a bomb calorimeter (PARR 6400) [16,17]. The thermal decomposition was evaluated by the calculated solid yield ($Y_{S,exp}$) and energy yield (Y_E) for the continuously weighted wood sample over time according to Eq. (1) and Eq. (2) respectively.

$$Y_{S,exp}(t) = \frac{m_i(t)}{m_0} \times 100 \qquad (1)$$

$$Y_E(t) = Y_{S,exp}(t) \times \frac{HHV_i}{HHV_0} \qquad (2)$$

where m_0 is the dried mass before torrefaction; m_i is the solid mass during torrefaction; HHV_0 is the higher heating value of untreated samples dry and ash-free basis; HHV_i is the higher heating value of torrefied samples dry and ash-free basi [16,17].

Statistical analyses were conducted using the Assistat 7.7 software [18]. Results for untreated and torrefied material were subjected to variance analysis (ANOVA) and the Tukey test at a 5% probability level. Six variables in response to the experiments were analyzed and discussed: the solid and energy yield (wt%), fixed carbon content (FC%), volatile matter content (VM%), ash content (Ash%), and the higher heating value (HHV) [16,17]. The general model for variance analysis was described by the Eq. (3):

$$Y_{ij} = \mu + [F_i + T_j + (F \times T)_{ij}] + \varepsilon_{ij} \qquad (3)$$

where Y_{ij} is the value observed for the dependent variable for observation ij, F is the acoustic frequency within the reactor, T the temperature, ε_{ij} is the error of the model and μ is a constant.

2.5 Kinetics modeling

The applied kinetic model to conduct the kinetic simulation was a three stage-approach kinetics model developed in [19–21]. The originally proposed by Di Blasi and Lanzetta (1997) [22] model lumped the torrefaction products into five pseudo-components:
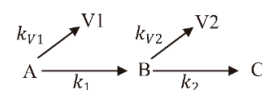
The time cumulative mass yield of the components is described by the sum of masses of A, B, and C, while the total mass of volatiles is described by the sum of V_1 and V_2 [19–21,23]. The four Arrhenius kinetic parameters (k_1, k_2, k_{V1}, k_{V2}) are determined by fitting predicted curves to experimentally measured TG curves [19]. The numerical calculation is performed using Matlab® to determine all kinetic parameters and the predicted solid yield $Y_{S,cal}(t) = A(t) + B(t) + C(t)$ [19–21]. The Eq. (4) describes the evolution of these pseudo components [19]:

$$\begin{cases} A(t) = \frac{dm_A(t)}{dt} = -(k_1 + k_{V1}) \times m_A(t) \\ B(t) = \frac{dm_B(t)}{dt} = k_1 \times m_A(t) - (k_2 + k_{V2}) \times m_B(t) \\ C(t) = \frac{dm_C(t)}{dt} = k_2 \times m_B(t) \\ V_1(t) = \frac{dm_{V1}(t)}{dt} = k_{V1} \times m_A(t) \\ V_2(t) = \frac{dm_{V2}(t)}{dt} = k_{V2} \times m_B(t) \end{cases} \quad (4)$$

Here, m_x is the mass of the pseudo component ($x = A, B, C, V_1, V_2$). The rate constant k_i (s^{-1}, $i = 1, 2, V_1, V_2$) obeying the Arrhenius law is calculated with Eq. (5) [19]:

$$k_i = k_{0,i} exp\left(\frac{-E_{a,i}}{RT}\right) \quad (5)$$

where $E_{a,i}$ (J.mol^{-1}) and $k_{0,i}$ (min^{-1}) are respectively the activation energies and the pre-exponential factors of the reactions, R is the universal gas constant (J.mol^{-1}.K^{-1}) and T is the absolute temperature (K) [19]:

3 RESULTS AND DISCUSSIONS

3.1 Acoustic torrefaction

The results of the proximate analyses for all the torrefied samples and summary statistics for the experimental factorial design performed are shown in Table III.

Table III: Properties of the torrefied solid with and without acoustic (Control). Classification by Tukey's test of averaged results considering three replicates per treatment. For each group, the means with the same letter were not significantly different at 5% ($\alpha = 0.05$).

Treatments		Proximate analyses (%)[*]		
T(°C)	Frequency	V.M	F.C	Ash
Raw.		81.4	46.03	0.09
250	**Control**	**77.17[a]**	**22.77[a]**	**0.054[a]**
	1411 Hz	76.69[a]	23.24[a]	0.067[a]
	1810 Hz	76.59[a]	23.35[a]	0.059[a]
	2478 Hz	77.40[a]	22.52[a]	0.082[a]
	2696 Hz	76.37[a]	23.56[a]	0.069[a]
270	**Control**	**71.12[b]**	**28.79[b]**	**0.086[b]**
	1411 Hz	71.21[b]	28.70[b]	0.094[b]
	1810 Hz	71.89[b]	28.02[b]	0.095[b]
	2478 Hz	71.14[b]	28.77[b]	0.093[b]
	2696 Hz	70.07[b]	29.81[b]	0.116[b]

V.M.: volatile matter; F.C.: fixed carbon. [*] Dry basis.

An analysis of variance (ANOVA) was carried out considering possible interactions between the two explanatory variables: acoustic frequencies (F) and temperature (T) [16,17]. When the temperature condition is assessed, a statistical significance is observed comparing 250 and 270 °C treatments, agreeing with [24,25] Considering the acoustic treatments for each temperature condition, the results had no significant differences between acoustic frequencies. The resulting values for ash content were inexpressive, even after the thermal treatment for both temperatures agreeing with [26] which obtained values close to 0% for the temperatures of 250 and 275 °C.

Table IV presents the energetic analysis results for the solid product. Considering the temperature assessment, the obtained results for energy yield showed a good agreement with the 90% (270 °C) energy yield obtained by Bergman et al. [27] and the 93.7 and 88.5 obtained by Lu et al. [26] at 250 and 275 °C respectively.

Table IV: Energy properties. Classification by Tukey's test of averaged results considering two replicates per treatment. For each group, the means with the same letter were not significantly different at 5% (α=0.05). Lowercase letters differ in the line and uppercase letters differ in the column. (Lowercase letters statistical difference in line and uppercase letters in the column).

	HHV (MJ.kg^{-1})		η_S (%)		η_E (%)	
	250°C	270°C	250°C	270°C	250°C	270°C
T1	**21.34[bB]**	**22.29[aC]**	**88.06[a]**	**81.29[b]**	**93.13[a]**	**90.09[b]**
T2	21.62[bA]	22.40[aAB]	87.43[a]	81.44[b]	94.02[a]	90.64[b]
T3	21.58[bA]	22.16[aD]	87.38[a]	80.81[b]	93.79[a]	89.61[b]
T4	21.57[bA]	22.33[aBC]	87.75[a]	81.43[b]	94.11[a]	90.65[b]
T5	21.53[bA]	22.43[aA]	87.54[a]	81.03[b]	93.86[a]	90.45[b]

T1: control; T2: 1411Hz; T3: 1810Hz; T4: 2478Hz; T5: 2696Hz.

A higher gain of HHV is usually associated with the percentage FC increasing [28]. According to Table III and IV treatments that had the highest percentage gains in FC also had higher gains in HHV, except for the treatment under 2478 Hz frequency at 250 °C temperature. Resulting values for treatments under acoustic influence were superior to the control (without acoustic), except for the frequency 1810 Hz at 270 °C.

Table IV shows that the best results for HHV occurred at 270 °C. At 250 °C temperature, the treatments with acoustics did not differentiate between them but were statistically better than the control. At the temperature of 270 °C, the treatments 2696 and 1411 Hz achieved the best results differing statistically from the control. The 1810 Hz frequency was the one that presented the lowest HHV value. In absolute values, the energy yields average for the acoustics treatments were higher than the control, both at the temperature 250 and 270 °C, except for the frequency 1810 Hz at 270 °C.

According to the analysis of variance in Table V, there was a statistical difference only for the temperature when evaluating the proximate analysis parameters (VM, FC and Ash content) and solid yield (η_S). For the energy yield (η_E), there was a statistical difference for both temperature and frequency and their interaction.

Thus, the 1411 and 2696 Hz treatments also showed to be statistically significant for HHV and energy values for 270 °C when compared to treatments without acoustic

and the other two frequencies (1810 and 2478 Hz) and were retained for more detailed analysis in Section 3.2.

Table V: Analysis of variance of the temperature (T) and the acoustic frequency (F) parameters, along with their first and second-order interactions for the six response variables. CV = Coefficient of variation; * = statistically significant; ns = not statistically significant at 1%. The values correspond to the F test.

Response variable	VM (%)	FC (%)	Ash (%)
T	373.785 *	350.124 *	46.238 *
F	1.714 ns	1.663 ns	3.092 ns
T x F	1.035 ns	1.005 ns	1.748 ns
CV (%)	1.2	4.06	19.5
	HHV	η_S (%)	η_E (%)
T	4133.566 *	3205.022*	835.068 *
F	34.968*	1.322 ns	6.981 *
T x F	27.762*	1.018 ns	2.385 ns
CV (%)	0.13	0.46	0.46

3.2 Optimum frequencies

The analysis showed that both frequencies 1411 and 2696 Hz presented the best results considering the energy properties of torrefied biomass. A deep analysis exploring treatment dynamics and chemical correlations diagrams was performed for the torrefied final product for these frequencies.

3.2.1 Solid yield and elemental analyses

Fig. 2 shows the obtained results in [14] for the solid yield evolution (a) and its derivative thermo-gravimetric (DTG) (b) for 250 and 270 °C treatments during experiments under 1411Hz and 2696 Hz acoustic influence with the same conditions (Table 2).
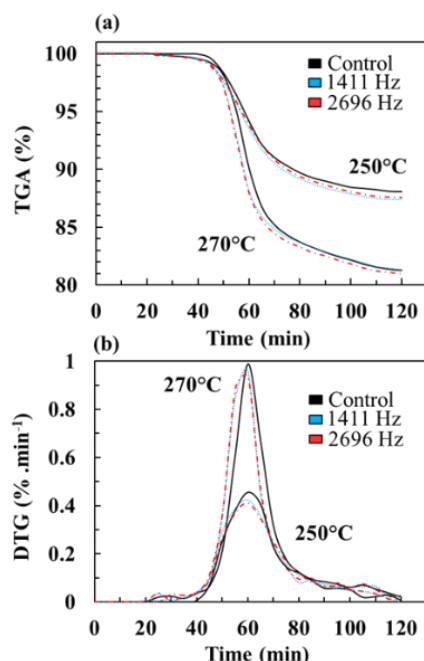

Figure 2: (a)TGA (%) and (b) DTG (g/min) for Control (no acoustic) and treatments with 1411 Hz and 2696 Hz frequencies performed at 250 °C and 270 °C.

For both 1411 and 2696 Hz frequencies, an anticipate degradation was evinced by a profile time shift [14]. This behavior was confirmed with an increased DTG profile showing faster conversion rates for treatments performed under acoustic for both temperatures [14].

Fig. 3 illustrates the listed values (Table III) of VM and FC contents (Fig. 3(a)), the atomic oxygen-to-carbon (O/C), and hydrogen-to-carbon (H/C) (Fig. 3(b)) for the control, 1411 and 2696 Hz frequencies. Raw biomass volatile matter content is higher when compared to treated wood, while its FC content is lower [1,25,29]. During biomass torrefaction, a dehydration process takes place releasing moisture and light volatiles from raw materials [1].
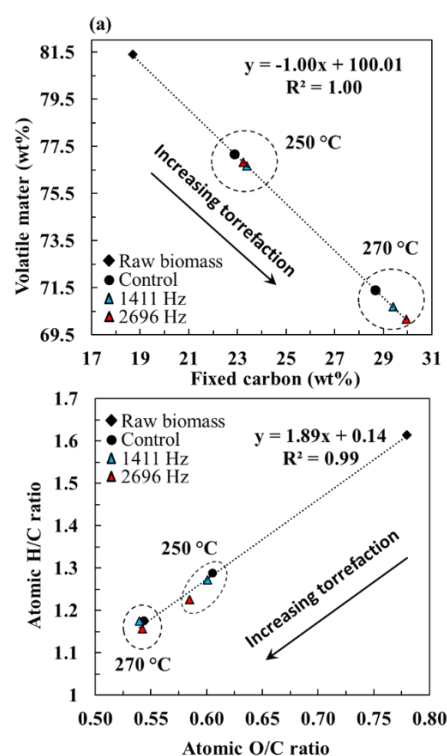

Figure 3: Results for fixed carbon (F.C) versus volatile matter (V.M) (a) and van Krevelen diagram (b) for optimum frequencies treatment (1411 and 2696 Hz).

The Van Krevelen diagram is illustrated in Fig. 3(b). After undergoing torrefaction, moisture and light volatiles, which contain more hydrogen and oxygen, are removed from biomass, whereas relatively more carbon is retained [1]. The obtained values for the atomic oxygen-to-carbon (O/C) and hydrogen-to-carbon (H/C) ratios for raw biomass and torrefied biomass showed a linear regression ($R^2 = 0.9976$) corroborated by the literature [1,25,30,31] Fig. 3(b) shows that the 2696 Hz treatment has a higher impact when compared to control and 1411 Hz frequency at 250 °C. For the 270 °C treatment, a not significant difference was reported.

3.2.2 Energy performance parameters

Fig. 4 displays the higher heating value (HHV) as a function of the solid yield (a) and de HHV enhancement (b) for treatments performed under 1411 Hz and 2696 Hz. Resulting values obtained for the raw material as well as for treatments performed with 250 and 270 °C agrees with the literature [14, 16, 17, 20]. Once they undergo standard

torrefaction, their HHV is increased to 21.33 and 22.29 for 250 and 270 °C respectively.

Comparing temperature (control) and coupled treatments (temperature and acoustic), it is possible to notice the same behavior for Fig. 4(a) and (b) where for the 250 °C temperature treatment coupled to 1411 Hz frequency a higher value for the HHV as well as for the HHV enhancement (solid bar) are reported. For the 270 °C temperature treatment, the 2696 Hz frequency had better results for both parameters.

From an industrial point of view, the ideal energy aspect is to obtain a high energy yield at a low solid volume (higher mass losses), dispending less energy during the pre-treatment process [26]. Lu et al. [26] determined an energy-mass co-benefit index (EMCI) that means the difference between the energy yield and the solid yield ($EMCI = \eta_E - \eta_S$). This INDEX was defined to seek the optimum condition operation between torrefaction treatments where a higher EMCI represents a better treatment to be applied to the raw material [26].
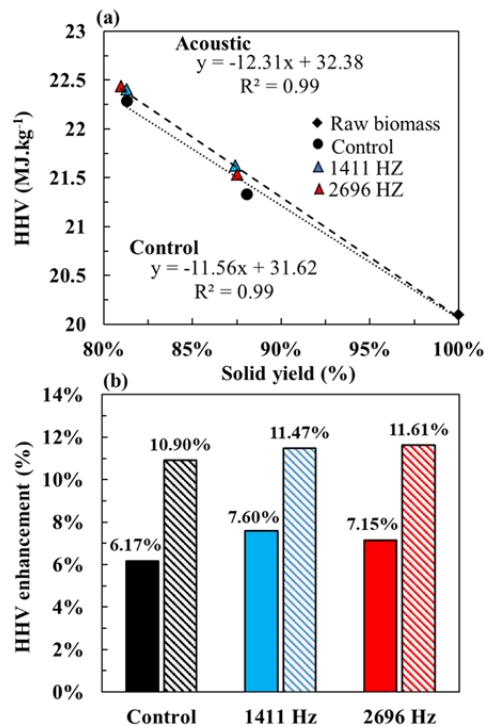

Figure 4: Higher heating value (HHV - MJ.kg-1) in function of the solid yield (%) (a) and de HHV enhancement (solid bar – 250 °C treatment, hatched bar – 270 °C treatment) (b) for the control and identified optimum treatments (1411 and 2696 Hz).

Fig. 5 illustrates the solid and energy yields and the calculated energy-mass co-benefit indexes (EMCI) of *Eucalyptus grandis* for torrefaction treatments under temperature influence and coupled temperature and frequencies (1411 and 2696 Hz). During torrefaction, the weight loss will lessen the energy yield, whereas the enhancement of HHV facilitates energy yield [1]. Seeing that the impact of the former on energy yield is over the latter, the energy yield decreases with increasing temperature and duration [1]. For 250 °C treatment, the bar chart in Fig. 5 shows a maximum value of 6.62 EMCI (1411 Hz treatment) and for 270 °C treatment a maximum value of 9.41 EMCI (2696 Hz) implying that optimum

operations occur at these conditions. This result agrees with the entire torrefied product assessment.
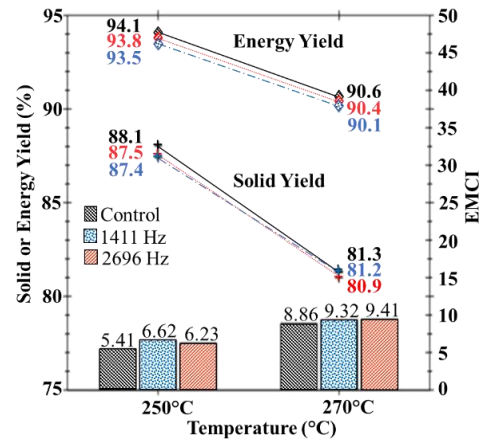

Figure 5: Solid and energy yields and energy-mass co-benefit indexes EMCI (bar chart) of eucalyptus for control (no acoustic) and 1411 and 2696 Hz acoustic treatment.

3.3 Thermo-acoustic kinetics simulation

The experimental data (Fig. 2) [14,17] from standard torrefaction (control) and for the identified optimum frequencies (1411 and 2696Hz) of the coupled thermo-acoustic torrefaction were used as input data. The resulting fitted curves are presented in Fig. 6.
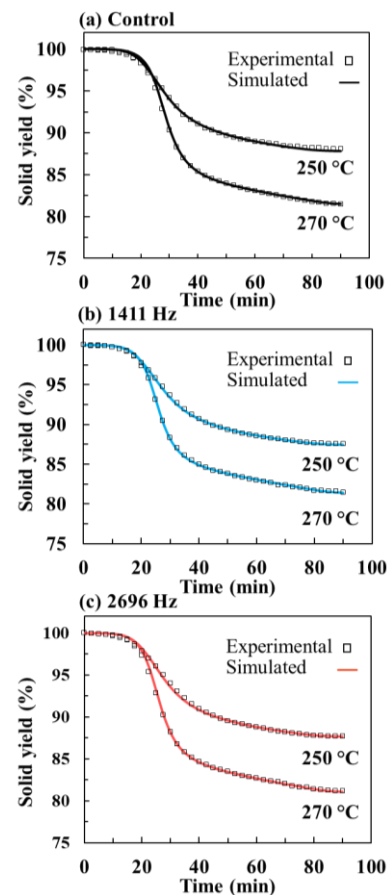

Figure 6: Simulated and experimental curves for control (a) and acoustic treatments (b) 1411 and (c) 2696Hz performed at 250 °C and 270 °C.

For a better convergence during the simulation the input data was established before the 170 °C temperature [19]. For the kinetics study, three sets of kinetic parameters groups $(k_1, k_{v1}, k_2, k_{v2})$ for control, 1441 and 2696Hz experiments were obtained for both temperatures (250 and 270°C). Fig. 6(a) present the fitted curves for experiments without acoustic (control) and 6(b) and (c) presented the fitted curves for 1411 and 2696Hz thermo-acoustic torrefaction respectively. The simulated curves from the obtained kinetic parameters present an accurate fitted for the three cases. The calculated kinetic rates with the obtained pre-exponential factors and activate energy are illustrated in Fig. 7.
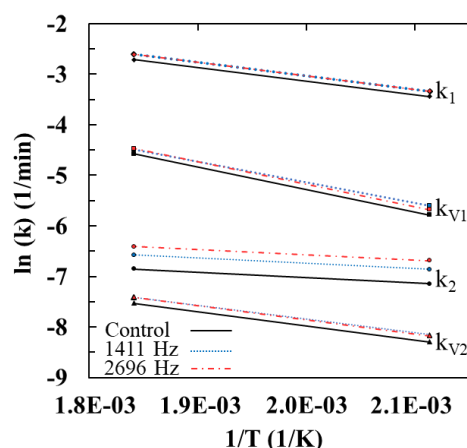

Figure 7: Simulation results for comparison of the reaction rates for control, 1411 and 2696Hz treatments.

As can be seen in Fig. 7 the same kinetics behavior (line slope) is obtained for all treatments, being those acoustic ones faster than the control. The obtained kinetics for the acoustic experiments presented very similar behavior showing fasters reaction rates in comparison to control (without acoustic) for the first step k_1, k_{v1}, as well as for the second step k_2, k_{v2}. Bates et Ghoniem (2013) reported in [33] that the faster first stage of torrefaction is primarily attributable to the decomposition of hemicellulose (with an increasing contribution from cellulose decomposition at higher temperatures). The mass loss during the second stage is primarily due to cellulose decomposition, with minor lignin decomposition and charring of the remaining hemicellulose [33].

An interesting resulting obtained in this investigation is that the parameter k_2, which represents the second stage of thermodegradation (remaining hemicelluloses and mainly the cellulose), had a higher displacement in comparison to the other kinetic parameters. The 2696Hz treatments presented the faster kinetics for this parameter.

4 CONCLUSIONS

This study presented the assessment of torrefied biomass obtained by coupling acoustic device with a conventional torrefaction reactor. Considering the acoustic torrefaction results, the final solid yields were very similar whatever the acoustic frequency, however, its dynamic profiles show that acoustic may accelerate the degradation process. The statistical analysis demonstrated significant differences for acoustic torrefied eucalyptus HHV. The numerical modeling showed the catalytic behavior with

faster kinetic parameter for acoustic tratments. The obtained results will guide further adjustments on torrefaction parameters, acoustic intensities and reactor design aiming an optimal upgrading in torrefaction process.

5 REFERENCES

[1] W.-H. Chen, J. Peng, X.T. Bi, A state-of-the-art review of biomass torrefaction, densification and applications, Renew. Sustain. Energy Rev. 44 (2015) 847–866. doi:10.1016/j.rser.2014.12.039.

[2] H.C. Ong, W.H. Chen, Y. Singh, Y.Y. Gan, C.Y. Chen, P.L. Show, A state-of-the-art review on thermochemical conversion of biomass for biofuel production: A TG-FTIR approach, Energy Convers. Manag. 209 (2020) 112634. doi:10.1016/j.enconman.2020.112634.

[3] M.N. Cahyanti, T.R.K.C. Doddapaneni, T. Kikas, Biomass torrefaction: An overview on process parameters, economic and environmental aspects and recent advancements, Bioresour. Technol. 301 (2020) 122737. doi:10.1016/j.biortech.2020.122737.

[4] D. Chen, F. Chen, K. Cen, X. Cao, J. Zhang, J. Zhou, Upgrading rice husk via oxidative torrefaction: Characterization of solid, liquid, gaseous products and a comparison with non-oxidative torrefaction, Fuel. 275 (2020) 117936. doi:10.1016/j.fuel.2020.117936.

[5] J.S. Tumuluru, S. Sokhansanj, J.R. Hess, C.T. Wright, R.D. Boardman, A review on biomass torrefaction process and product properties for energy applications, Ind. Biotechnol. 7 (2011) 384–401. doi:10.1089/ind.2011.0014.

[6] T.A. Mamvura, G. Danha, Biomass torrefaction as an emerging technology to aid in energy production, Heliyon. 6 (2020) e03531. doi:10.1016/j.heliyon.2020.e03531.

[7] M. Carrier, A.G. Hardie, Ü. Uras, J. Görgens, J. Knoetze, Production of char from vacuum pyrolysis of South-African sugar cane bagasse and its characterization as activated carbon and biochar, J. Anal. Appl. Pyrolysis. 96 (2012) 24–32. doi:10.1016/j.jaap.2012.02.016.

[8] M. Garcìa-Pérez, A. Chaala, H. Pakdel, D. Kretschmer, C. Roy, Vacuum pyrolysis of softwood and hardwood biomass. Comparison between product yields and bio-oil properties, J. Anal. Appl. Pyrolysis. 78 (2007) 104–116. doi:10.1016/j.jaap.2006.05.003.

[9] Q.V. Bach, K.Q. Tran, Ø. Skreiberg, Comparative study on the thermal degradation of dry- and wet-torrefied woods, Appl. Energy. 185 (2017) 1051–1058. doi:10.1016/j.apenergy.2016.01.079.

[10] Q.V. Bach, O. Skreiberg, Upgrading biomass fuels via wet torrefaction: A review and comparison with dry torrefaction, Renew. Sustain. Energy Rev. 54 (2016) 665–677. doi:10.1016/j.rser.2015.10.014.

[11] L.A. de Macedo, J.M. Commandré, P. Rousset, J. Valette, M. Pétrissans, Influence of potassium carbonate addition on the condensable species released during wood torrefaction, Fuel Process. Technol. 169 (2018) 248–257. doi:10.1016/j.fuproc.2017.10.012.

[12] M. Safar, B.-J.J. Lin, W.-H.H. Chen, D. Langauer,

J.-S.S. Chang, H. Raclavska, A. Pétrissans, P. Rousset, M. Pétrissans, Catalytic effects of potassium on biomass pyrolysis, combustion and torrefaction, Appl. Energy. 235 (2019) 346–355. doi:10.1016/j.apenergy.2018.10.065.

[13] H.C. Ong, W.H. Chen, A. Farooq, Y.Y. Gan, K.T. Lee, V. Ashokkumar, Catalytic thermochemical conversion of biomass for biofuel production: A comprehensive review, Renew. Sustain. Energy Rev. 113 (2019) 109266. doi:10.1016/j.rser.2019.109266.

[14] E.A. Silveira, M.V.G. de Morais, P. Rousset, A. Caldeira-Pires, A. Pétrissans, L.G.O. Galvão, Coupling of an acoustic emissions system to a laboratory torrefaction reactor, J. Anal. Appl. Pyrolysis. 129 (2017) 29–36. doi:10.1016/j.jaap.2017.12.008.

[15] G.D. Rosseto, Contribution to the theory and practice of experimental acoustical modal analysis, Universidade Estadual de Campinas, 2001. http://repositorio.unicamp.br/jspui/handle/REPOSIP/265319.

[16] Luiz Gustavo Oliveira Galvão, Efeitos da acústica e da temperatura no processo de torrefação e nas propriedades energéticas da madeira de eucalyptus grandis, University of Brasília, 2018. http://repositorio.unb.br/handle/10482/32315.

[17] E.A. Silveira, Acoustic field influence in the kinetics of thermochemical degradation during biomass torrefaction, 2018. https://tel.archives-ouvertes.fr/tel-01886056.

[18] de A.S. e S. Francisco, A.V. de A. Carlos, The Assistat Software Version 7.7 and its use in the analysis of experimental data, African J. Agric. Res. 11 (2016) 3733–3740. doi:10.5897/AJAR2016.11522.

[19] E.A. Silveira, B.J. Lin, B. Colin, M. Chaouch, A. Pétrissans, P. Rousset, W.H. Chen, M. Pétrissans, Heat treatment kinetics using three-stage approach for sustainable wood material production, Ind. Crops Prod. 124 (2018) 563–571. doi:10.1016/j.indcrop.2018.07.045.

[20] B.J. Lin, E.A. Silveira, B. Colin, W.H. Chen, Y.Y. Lin, F. Leconte, A. Pétrissans, P. Rousset, M. Pétrissans, Modeling and prediction of devolatilization and elemental composition of wood during mild pyrolysis in a pilot-scale reactor, Ind. Crops Prod. 131 (2019) 357–370. doi:10.1016/j.indcrop.2019.01.065.

[21] B.J. Lin, E.A. Silveira, B. Colin, W.H. Chen, A. Pétrissans, P. Rousset, M. Pétrissans, Prediction of higher heating values (HHVs) and energy yield during torrefaction via kinetics, in: Energy Procedia, 2019: pp. 111–116. doi:10.1016/j.egypro.2019.01.054.

[22] C. Di Blasi, M. Lanzetta, Intrinsic kinetics of isothermal xylan degradation in inert atmosphere, J. Anal. Appl. Pyrolysis. 40–41 (1997) 287–303. doi:10.1016/S0165-2370(97)00028-4.

[23] R.B. Bates, A.F. Ghoniem, Biomass torrefaction: Modeling of volatile and solid product evolution kinetics, Bioresour. Technol. 124 (2012) 460–469. doi:10.1016/j.biortech.2012.07.018.

[24] P. Rousset, L. MacEdo, J.M. Commandré, a. Moreira, Biomass torrefaction under different oxygen concentrations and its effect on the composition of the solid by-product, J. Anal. Appl. Pyrolysis. 96 (2012) 86–91. doi:10.1016/j.jaap.2012.03.009.

[25] S.W. Park, C.H. Jang, K.R. Baek, J.K. Yang, Torrefaction and low-temperature carbonization of woody biomass: Evaluation of fuel characteristics of the products, Energy. 45 (2012) 676–685. doi:10.1016/j.energy.2012.07.024.

[26] K.M. Lu, W.J. Lee, W.H. Chen, S.H. Liu, T.C. Lin, Torrefaction and low temperature carbonization of oil palm fiber and eucalyptus in nitrogen and air atmospheres, Bioresour. Technol. 123 (2012) 98–105. doi:10.1016/j.biortech.2012.07.096.

[27] P.C. a. Bergman, J.H. a. Kiel, Torrefaction for biomass upgrading - ręczne notatki, Proc. 14th Eur. Biomass Conf. Paris, Fr. (2005) 17–21. http://scholar.google.com/scholar?hl=en&btnG=Search&q=intitle:Torrefaction+for+biomass+upgrading#0.

[28] J. Parikh, S.A. Channiwala, G.K. Ghosal, A correlation for calculating HHV from proximate analysis of solid fuels, Fuel. 84 (2005) 487–494. doi:10.1016/j.fuel.2004.10.010.

[29] G. Almeida, J.O. Brito, P. Perré, Alterations in energy properties of eucalyptus wood and bark subjected to torrefaction: The potential of mass loss as a synthetic indicator, Bioresour. Technol. 101 (2010) 9778–9784. doi:10.1016/j.biortech.2010.07.026.

[30] P. McKendry, Energy production from biomass (part 1): overview of biomass, Bioresour. Technol. 83 (2002) 37–46. doi:10.1016/S0960-8524(01)00118-3.

[31] E. Peduzzi, G. Boissonnet, G. Haarlemmer, C. Dupont, F. Maréchal, Torrefaction modelling for lignocellulosic biomass conversion processes, Energy. 70 (2014) 58–67. doi:10.1016/j.energy.2014.03.086.

[32] T.O. Rodrigues, P.L.A. Rousset, Effects of torrefction on energy properties of Eucalyptus grandis wood, Cerne. 15 (2009) 446–452. doi:10.1017/CBO9781107415324.004.

[33] R.B. Bates, A.F. Ghoniem, Biomass torrefaction: modeling of reaction thermochemistry., Bioresour. Technol. 134 (2013) 331–40. doi:10.1016/j.biortech.2013.01.158.

6 ACKNOWLEDGEMENTS